Theoretical study of the molecular and electronic structure of methanol on a TiO_2(110) surface

Jin Zhao,[1] Jinlong Yang,[2] and Hrvoje Petek[1]
[1]*Department of Physics and Astronomy and Petersen Institute of NanoScience and Engineering, University of Pittsburgh, Pittsburgh, Pennsylvania 15260, USA*
[2]*Hefei National Laboratory for Physical Sciences at Microscale, University of Science and Technology of China, Hefei, Anhui, China*
(Received 30 June 2009; revised manuscript received 10 September 2009; published 10 December 2009)

We present density-functional-theory calculations of the molecular and electronic structure of methanol adsorption on stoichiometric TiO_2(110) surface. We have investigated 11 different molecular and dissociated adsorption structures of CH_3OH at 1 monolayer coverage. The relative stabilities of different structures depend on the chemisorption-induced charge transfer, the relative strengths of different types of hydrogen bonds, the steric hindrance between methyl groups and the surface stress. We found the intermolecular hydrogen bonding to play an important role in stabilizing the overlayer. We also investigated the occupied and unoccupied surface electronic structure, and the adsorbate-induced surface dipole moment and work-function changes. The electronic structures show that the highest-occupied molecular orbital of CH_3OH is near the valance-band maximum, which reflects the character of CH_3OH as a hole scavenger on TiO_2 surfaces. The unoccupied partially solvated or "wet" electron states for CH_3OH on TiO_2 are primarily distributed on H atoms of methyl groups. Despite many different structural motifs, the wet-electron-state energy primarily correlates with the surface dipole moment.

DOI: 10.1103/PhysRevB.80.235416 PACS number(s): 68.43.Bc, 73.20.Hb, 68.43.Fg

I. INTRODUCTION

TiO_2 is a large band-gap semiconductor with a wide range of applications including in photocatalysis, decontamination, and solar-energy conversion.[1–7] The generation of electron-hole pairs by band-gap excitation with near-ultraviolet light can instigate the decomposition of organic molecules adsorbed on TiO_2 surfaces. As one of the simplest organic molecules, methanol adsorbed on TiO_2 surfaces has been intensively investigated by both experiment and theory in the context of catalysis and photocatalysis.[8–24] Methanol can adsorb on TiO_2 surfaces either molecularly or dissociatively. Scanning tunneling microscopy (STM) and temperature-programmed desorption (TPD) measurements show that the dissociation of CH_3OH is exothermic at oxygen-atom vacancies on reduced TiO_2 surfaces.[11,12,16,21] Also, chemical and TPD studies have been interpreted in terms of the partial CH_3OH dissociation on the stoichiometric TiO_2(110) surface whereby a proton is transferred from OH of methanol to bridging surface O atom of the surface to form a methoxy and an OH species.[12,16,21] The structure of CH_3OH on TiO_2 is complicated, as we will show by density-functional-theory (DFT) calculations; many distinct molecular and dissociative structures can coexist on account of both the intermolecular or molecule-surface hydrogen bonding with nearly equal chemisorption enthalpies.[8,17,22] In part because of this complexity, the precise understanding of the adsorption structure of CH_3OH on the most extensively studied rutile TiO_2(110) surface is still lacking.

In order to understand the photocatalytic activity of methanol it is also important to determine how it interacts with photogenerated electrons and holes. In the photocatalysis literature it is well established that methanol acts as a hole trap,[10] and a sacrificial agent in the photocatalytic production of H_2.[25,26] To best of our knowledge, however, there have neither been studies to determine the nature of the methanol-hole interaction nor has it been established whether holes interact more strongly with the molecular or the deprotonated form.

The situation is different for photogenerated electrons, for which the interaction with protic solvents has been studied through a joint time-resolved two-photon photoemission (TR-2PP) spectroscopy and DFT electronic-structure investigation. These studies discovered the two-dimensional (2D) partially solvated electron states at the H_2O/TiO_2 and CH_3OH/TiO_2 interfaces.[19,27,28] The idea of surface-solvated electron state, which was dubbed the "wet-electron state,"[29] comes from the studies of excess electrons bound by dipolar forces to surfaces of small $(H_2O)_n^-$ $(n \geq 2)$ clusters.[29–40] Solvated electrons in protic solvents are one of the most fundamental chemical reagents of significant interest in many physical and chemical contexts.[29–35,37,38,40–49] In $(H_2O)_n^-$ clusters, dangling H atoms, which do not participate in strong hydrogen bonds (HBs), present the most electrophilic acceptor sites for stabilizing excess electrons.[29,35,50,51] Yet most experimental and theoretical studies of solvated electrons have focused on the liquid phase or on systems consisting of small to intermediate size protic solvent anion clusters. In more recent TR-2PP studies, Wolf and coworkers have studied solvation of electrons injected into the conduction bands (CBs) of H_2O and NH_3 multilayers on metal surfaces. In these studies as well, the dangling H atoms at the adsorbate vacuum interface have been proposed as the primary electron solvation sites.[52–55]

2PP spectra for H_2O/TiO_2 surface show a resonance 2.4 eV above the Fermi level (E_F) that can act as an intermediate level in two-photon photoemission process. Based on chemical evidence and DFT calculations, we attributed this resonance to the 2D wet-electron states. An electron transiently occupying the wet-electron state decays back to the CB through resonant charge transfer (RCT) with a lifetime of ~15 fs.[56] As in $(H_2O)_n^-$ clusters and H_2O multilayers on

metals, the DFT calculations show that the 2D wet-electron state is also stabilized by the dangling H atoms.[27] Because the H atoms of H_2O molecules on the stoichiometric TiO_2 surface are engaged in favorable HBs, however, the 2.4 eV resonance primarily corresponds to electrons stabilized by the minority bridging hydroxyl (OH_b) species. The OH_b species form through the dissociation of water molecules at the bridging oxygen (O_b) vacancies on the partially reduced TiO_2 surfaces. These highly reactive O_b vacancy defects form under reducing conditions on TiO_2(110) surfaces.[4,12,57] From these experimental and theoretical studies we concluded that (i) the wet-electron-state energy depends on the H_2O-molecule coverage and chemisorption structure; (ii) they have one-dimensional or 2D character depending on the templated growth of H_2O molecules on the metal-oxide substrate [e.g., on TiO_2(110)-surface H_2O molecules form linear chains]; (iii) they present the lowest-energy pathway for the nonadiabatic electron transfer at metal-oxide/aqueous interfaces; and (iv) they may participate in photocatalytic reduction processes on metal-oxide surfaces.[28]

Encouraged by the results on H_2O/TiO_2, we performed similar experiments and calculations on CH_3OH adsorbed on TiO_2(110) surface.[19,56] In close correspondence with the H_2O case, an analogous wet-electron state appears 2.3 eV above the E_F. By contrast to the H_2O case, however, the lifetime of wet electrons at CH_3OH/TiO_2 interface can extend to >100 fs time scale depending on the molecular coverage and deuterium isotope (CH_3OD) substitution. The dynamical response reveled by TR-2PP showed that both the wet-electron population and its average energy relative to E_F decay in a biphasic manner; we assigned the initial 30–40 fs time-scale process to inertial solvation that stabilizes the wet-electron state with respect to RCT; and a longer 100 fs to picosecond time-scale component to diffusive solvation, which further stabilizes the injected electrons within the CH_3OH overlayer. Surprisingly, this latter component has a factor of 2.2 slower decay rate for the equivalent CH_3OD overlayer. We attributed the deuterium isotope effect to proton-coupled electron transfer based on a Δ-SCF calculation, which indicated how the overlayer response, involving hydrogen bond (HB) breaking and methanol OH deprotonation, might stabilize the wet-electron state.[19,28] Thus, TR-2PP studies along with DFT calculations on CH_3OH/TiO_2 provide molecular-level insights into the photophysical and photochemical processes, which are initiated by the optical injection of electrons into the wet-electron states. Therefore, there is a strong motivation to study in greater detail both the diversity of chemisorption structures of CH_3OH/TiO_2 interface and how they interact with the photogenerated carriers.

Here, we calculate by DFT 11 different chemisorption structures of 1 monolayer (ML) CH_3OH on stoichiometric rutile TiO_2(110) surface. We report the structure-dependent chemisorption energies, the overlayer electronic structures, surface-adsorbate charge-transfer properties, and surface dipole moments. The properties of wet-electron states for different adsorption structures and their correlation with the electrostatic properties of the interface also are discussed in detail.

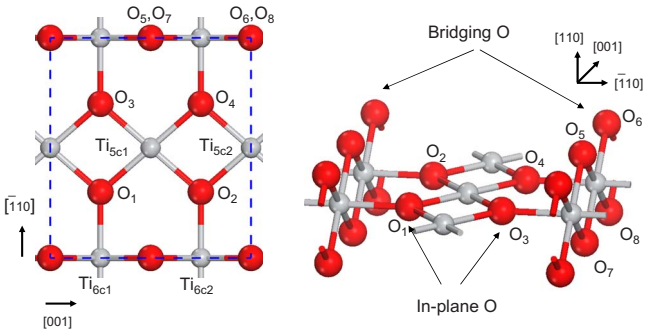

FIG. 1. (Color online) The structure of the TiO_2(110) surface. Small gray and large red spheres indicate the titanium and oxygen ions. O_1-O_4 are the O_{3c} atoms, and O_5 and O_6 are the bridging O atoms. (a) Top view of the (2×1) surface unit cell. (b) Side view showing the slab geometry.

II. COMPUTATIONAL METHODS

Plane-wave pseudopotential DFT calculations are used to characterize various optimized molecular structures of CH_3OH chemisorption on TiO_2(110) surface. The calculations are carried out with the "Vienna *ab initio* simulation package code" (VASP).[38–40] The O 1*s* and Ti 1*s* to 3*p* electrons are treated as core states. The generalized gradient approximation (GGA) with the spin-polarized Perdew-Burke-Ernzerhof functional[58] and the projector-augmented wave potential are used for all of the calculations.[59]

The surface is modeled with slabs cut out of a TiO_2 crystal to expose the (110) surface. As shown in Fig. 1, TiO_2(110) surface contains five- and six-coordinate Ti atoms (Ti_{5c} and Ti_{6c}), and two- and three-coordinate O atoms. Above the surface plane, the two-coordinate O atoms bond to the Ti_{6c} atoms forming the so-called bridging oxygen rows. The periodically repeated slabs are decoupled by 10 Å vacuum gaps. A Monkhorst-Pack grid of $(3\times3\times1)$ *k* points is used for the (2×1) surface unit cell. The molecules are adsorbed on both sides of the slab. The positions of all atoms are allowed to relax until the force acting on each is less than 0.02 eV $Å^{-1}$. We use a 400 eV plane-wave cutoff for optimization of the molecular structure and a 520 eV cutoff for the static calculations of the electronic structure.

III. RESULTS

A. CH_3OH adsorption structure

We investigated different adsorption structures of 1 ML CH_3OH on TiO_2(110) surface. We define 1 ML coverage by 100% occupation of Ti_{5c} sites by CH_3OH molecules. According to our calculations, for 1 ML coverage, two CH_3OH molecules can adsorb for each TiO_2(110) (2×1) surface unit cell, despite the likely steric hindrance between the adjacent methyl groups.[12]

Like H_2O, on the stoichiometric TiO_2-surface CH_3OH adsorbs preferentially with its O atom forming a bond with Ti^{4+} ions at Ti_{5c} sites. The H atom of OH can form either molecule-surface or intermolecular HB. Moreover, there is evidence that methanol can deprotonate at OH to form a methoxy at Ti_{5c} site and OH_b species on the O_b rows.[12,21] We

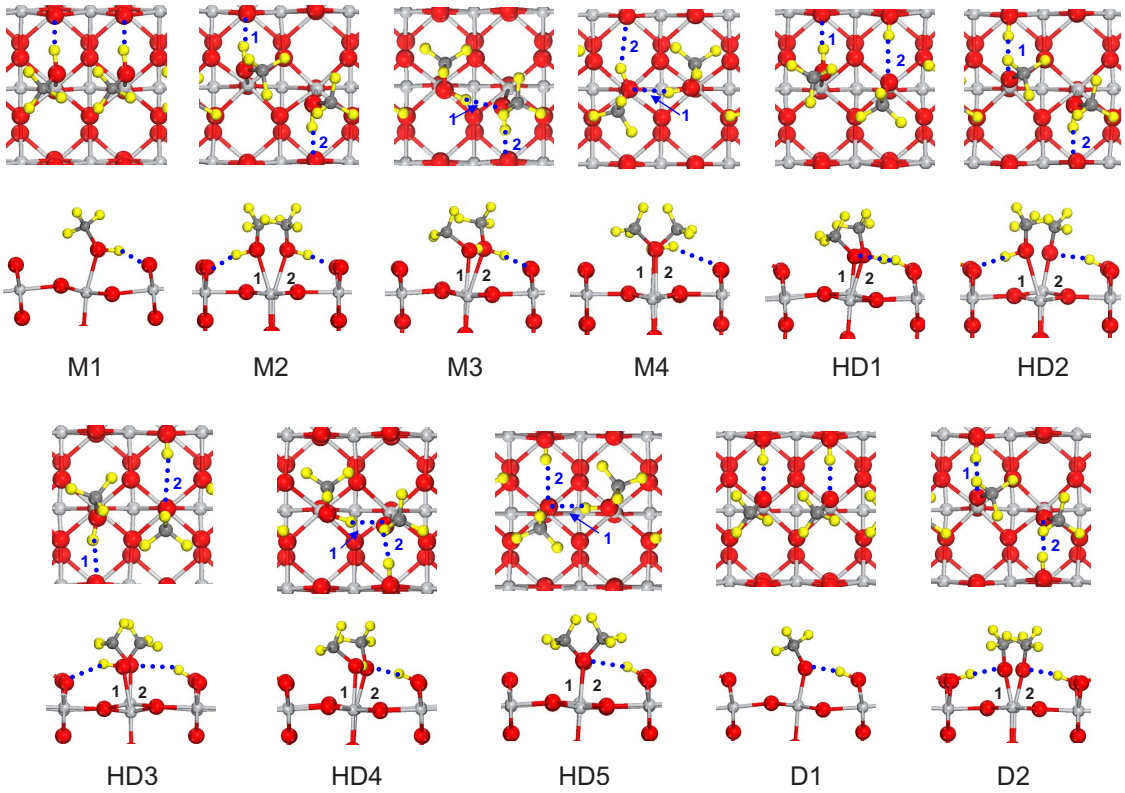

FIG. 2. (Color online) The top and side views of 11 different optimized adsorption structures for 1 ML coverage with one CH_3OH molecule at each Ti_{5c} site on the (2×1) surface unit cell. The blue doted lines indicate the hydrogen bonds and the numbering identifies the specific bonds that are compared in Table I.

have investigated 2×1 surface unit-cell structures where both CH_3OH molecules adsorb molecularly, one of the two molecules within the unit-cell deprotonates, and both molecules deprotonate (Fig. 2). We also investigated a proposed additional adsorption site for a (3×1) unit cell where in order to relive steric hindrance one of the two CH_3OH molecules in the unit cell is located at a bridging site between two Ti_{5c} atoms and the other is on top of the remaining Ti_{5c} site; such structure has been proposed to rationalize why in TPD measurements 1 ML coverage corresponds to the occupation of 70% of Ti_{5c} sites.[12]

Figure 2 shows the optimized structures of 11 distinct stable adsorption configurations that we have studied. We identified four molecular structures (M1–M4), five half-dissociated structures (HD1–HD5), and two fully dissociated structures (D1 and D2). The bridging site between two Ti_{5c} sites was found to be unstable with respect to adsorption on top of Ti_{5c} sites. Therefore, for the theoretical structures the steric hindrance does not prevent CH_3OH molecules from occupying each Ti_{5c} site.

The M1 molecular adsorption structure has two methanol molecules oriented in the same direction and adsorbed on each Ti_{5c} atom in the 2×1 surface unit cell. The hydroxyl H atoms form HBs with the neighboring O_b atoms. M2 is similar to M1 but the two methanol molecules are oriented in the opposite direction to form HBs to the opposing O_b-atom rows. This allows the methyl groups to adopt different configurations than in M1, thereby reducing the steric hindrance between them. In the M3 and M4 structures, one molecule within the unit cell forms an HB to the proximate O_b atom while the other molecule interacts with the first molecule through an intermolecular HB. Even though the most stable structure is M3 according to our calculations, as far as we know, such intermolecular bonding structures have not been previously studied by theory. The HD1 and HD2 structures are based on the M1 and M2 structures, respectively, where one H atom is transferred within the existing HB from CH_3OH to O_b atom to form the corresponding HB between OH_b and O atom of methoxy formed at the Ti_{5c} site. The HD3 structure is similar to HD2, however, each methyl group points in a different direction, as shown in Fig. 2. The HD4 and HD5 structures are obtained from the M3 and M4 structures by transferring the H atom to O_b site within the molecule-surface HB. The D1 and D2 structures are the two fully deprotonated M1 and M2 structures.

Because it has been shown that the molecular adsorption energies on TiO_2 surfaces have significant dependence on the slab thickness, we have investigated the methanol adsorption energy as a function of the number of O-Ti-O layers in a slab. The adsorption energies E_{ads} are defined by $E_{ads}=1/n[E_{CH_3OH/TiO_2}-(E_{TiO_2}+nE_{CH_3OH})]$, where E_{TiO_2} and E_{CH_3OH} are the total energies of the clean surface and free CH_3OH molecule and n is the number of CH_3OH molecules within the unit cell. The higher E_{ads} corresponds to a more stable structure. Figure 3 gives the layer-number-dependent adsorption energy for different structures. As reported previously, the adsorption energies oscillate between the odd and even number of layers and converge slowly as the number of

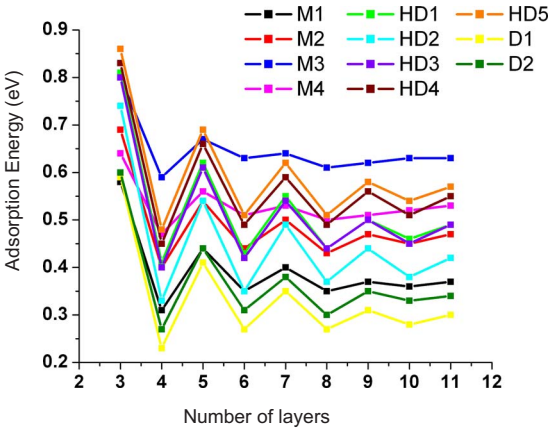

FIG. 3. (Color online) The adsorption energy dependence on the slab thickness for the different adsorption structures in Fig. 2.

layers is increased.[17,60–65] In order to get reliable adsorption energies, we have studied up to 11-layer thick slabs, for which the energy difference with respect to the corresponding ten-layer slab is smaller than 0.03 eV. We have also checked how treating the $3p$ electrons of Ti as valance electrons affects adsorption energies. Based on 11-layer calculations of the M3, HD4, and D1 structures, we found that the adsorption energy decreases by only 0.04–0.06 eV, in agreement with trends reported by Deskins.[66] Moreover, the order of stability of different structures does not depend on the basis set.

The molecular M3 structure, with adsorption energy of 0.63 eV, is the most stable one we found. As already pointed out, this structure has one intermolecular and one molecule-surface HB, indicating that both kinds of HBs need to be considered to understand the chemisorption of CH_3OH on TiO_2. In agreement with this finding, the HD5, HD4, and M4 structures, which also have intermolecular HBs, are more stable than the other structures with only molecule-surface HBs. The two fully dissociated structures D1 and D2 have the lowest E_{ads} of 0.30 and 0.34 eV, respectively. Thus, we also conclude that for $CH_3OH/TiO_2(110)$ surface the molecular chemisorption is favored over the partially or fully dissociated forms. In reality, however, both species are likely to exist on $TiO_2(110)$ surface.

The chemisorption of CH_3OH on TiO_2 can be understood by elaborating the adsorbate-substrate charge transfer. Substantial charge transfer is evident from the adsorbate-induced work-function change in 2PP spectra of CH_3OH-covered TiO_2 surfaces, which will be calculated in due course.[18,56] Figure 4 presents the spatial distribution of charge transfer upon CH_3OH adsorption on $TiO_2(110)$ surface for three representative structures. The charge densities of the donor ρ_+ and acceptor ρ_- sites are defined by the difference $\rho_\pm = \pm(\rho_{TiO_2}+\rho_{CH_3OH}-\rho_{CH_3OH/TiO_2})$ between the noninteracting surface and adsorbate and the chemisorbed state. We have also performed Bader charge analysis of the electron density, which is reported in Table S1 of the supplementary materials,[67] in order to get numerical atomic-level charge-transfer information. From the charge redistribution and Bader analysis, we gain insight into the molecule-surface bond formation. For the M3, HD4, and D1 structures in Fig.

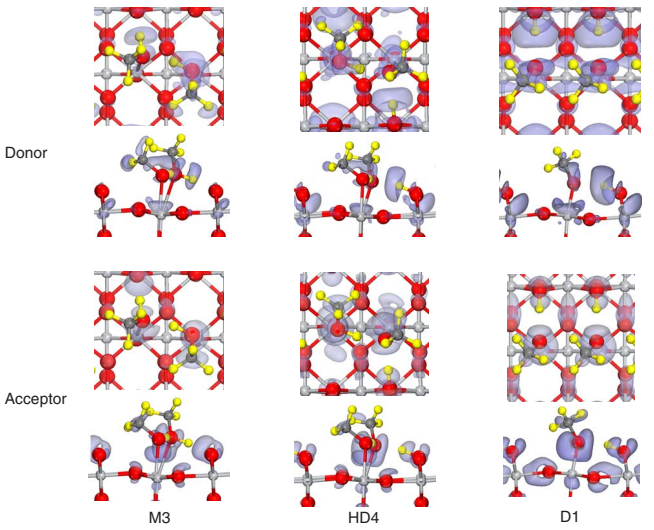

FIG. 4. (Color online) Top and side views of the donor and acceptor charge-transfer spatial distributions for the M3, HD4, and D1 structures.

4 we conclude that upon forming Ti-O bond there is charge transfer from Ti_{5c} atom and as well as methyl group to O atom of methanol or methoxy. The net positive charge on Ti_{5c} and negative charge on O of the adsorbate is the basis for the partially ionic Ti-O bond. For the molecularly adsorbed CH_3OH, there is also charge transfer from H of OH group to surface O_b upon forming the molecule-surface HB. For the deprotonated structures, there is charge transfer within the molecule-surface HB from the H atom of OH_b species to the O atom of methoxy. In the intermolecular HBs, charge is transferred from H atom of OH on one molecule to O atom of the neighboring molecule. There is also substantial charge transfer to O_{3c} sites of the surface, especially in the proximity of methoxy species. Finally, charge is transferred from above to below Ti_{5c} sites upon coordination with methanol or methoxy.

Several factors that can affect the relative stability of different adsorption structures include the strengths of bonds between the adsorbate and substrate (Ti_{5c}-O and HB), the relative strengths of the intermolecular versus molecule-substrate HBs, the relative stabilities of the molecular and deprotonated forms, the steric hindrance between the methyl groups, and the adsorbate-induced lattice strain.[68] Table I gives the Ti-O and HB lengths of the optimized adsorption structures from the 11-layer slab calculations. We found that the intermolecular HBs are always quite strong as judged by their lengths, which vary from 1.49 to 1.67 Å. This is shorter than 1.80 Å for the corresponding intermolecular HBs calculated for 1 ML of H_2O on $TiO_2(110)$ surface.[27] These strong intermolecular HBs appear to be responsible for the particular stability of the structures that posses them. Because of the steric hindrance between the methyl groups, however, initial structures in DFT calculations with two intermolecular HBs are not stable and converge to either the M3 or M4 structures. Therefore, we do not expect methanol to form linear hydrogen-bonded chains as proposed for CH_3OH in the liquid phase and anion clusters.[69] The role of steric interactions can be further appreciated if we compare

TABLE I. The adsorption energy, the Ti-O and hydrogen bond lengths, the work-function change, the relative surface dipole moment, the wet-electron-state energy relative to CBM, and the CH_3OH (OCH_3) HOMO energy (E_{HOMO}) relative to VBM, are given for different adsorption structures. The reference energies for the wet-electron state and CH_3OH HOMO (OCH_3) are the CBM and VBM, respectively. The numbering of H and O atoms is specified in Fig. 2.

	E_{ads} (eV)	O-$H_{(1)}$ (Å)	O-$H_{(2)}$ (Å)	Ti-$O_{(1)}$ (Å)	Ti-$O_{(2)}$ (Å)	$\Delta\varphi$ (eV)	Δp (10^{-3} e/Å)	E_{wet} (eV)	E_{HOMO} (eV)
M1	0.37	1.71		2.23		−2.25	5.5	2.70	−0.58
M2	0.47	1.62	1.62	2.35	2.35	−1.89	1.8	2.98	−0.47
M3	0.63	1.63	1.56	2.25	2.63	−2.14	6.1	2.79	−0.46
	(0.59)[a]								
M4	0.53	1.67	2.42	2.42	2.39	−2.51	8.2	2.40	−0.46
HD1	0.49	1.62	1.96	1.87	2.27	−1.96	3.0	2.90	−0.32
HD2	0.42	1.67	1.94	2.43	1.85	−2.08	5.6	2.78	−0.43
HD3	0.50	2.15	2.22	2.23	1.87	−2.30	7.8	2.54	−0.41
HD4	0.55	1.49	1.58	2.19	2.07	−1.76	1.2	3.13	−0.40
	(0.49)[a]								
HD5	0.57	1.49	2.00	2.20	2.00	−1.63	1.0	3.13	−0.27
D1	0.30	1.80		1.89		−1.60	0.0	3.26	−0.21
	(0.26)[a]								
D2	0.34	1.88	1.90	1.86	1.87	−1.97	4.0	2.90	−0.17

[a]Calculated with pseudopotential that treats Ti 3*p* as valence electrons.

the E_{ads} of M1 with M2 (or D1 with D2); methyl groups pointing in different directions minimize the steric hindrance leading to higher stability. Another aspect, which affects the adsorption energy, is the distortion of the TiO_2 lattice. In Table S2 of the supplementary materials we give the displacements of the surface-layer Ti and O atoms for 11-layer slab calculations for M3, HD4, and HD5 structures with respect to the optimized structure of the bare 11-layer thick slab. We notice that for the HD4 and HD5 structures, the distortion of the surface layer is stronger than for the M3 structure. The strong lattice distortion is caused by the methoxy group, which has a Ti-O bond that is substantially shorter (1.8–2.1 Å) than the corresponding methanol bond (2.2–2.4 Å), and also induces stronger charge transfer to the substrate. The cost of the lattice distortion, however, may explain in part why the M3 structure has a lower energy than the HD4 and HD5 structures.

In addition to the structures reported in Fig. 2 and Table I, we investigated several HD structures where H of OH_b has transferred to the neighboring O_b site whereby the methanol molecules form two HBs and the methoxy has no HBs. These structures have similar adsorption energies as the reported HD structures but otherwise do not provide additional insights into CH_3OH chemisorption.

B. Electronic structure

We have also investigated the electronic structure of $CH_3OH/TiO_2(110)$ surface. In Fig. 5 we plot the total density of states (DOS) and its projection onto the adsorbed CH_3OH molecule for the representative M3, HD4, and D1 structures. The energy is reported with respect to the conduction-band minimum (CBM). To establish the correct reference energy for the comparison of the unoccupied DOS at the surface from DFT calculations with that from 2PP experiments, we note that infrared-absorption and conductivity measurements locate $E_F \sim 120$ meV below the CBM for mildly reduced rutile TiO_2.[19,56,70–72] As is expected for DFT calculations, the calculated band gap of TiO_2 with the GGA functional is around 1.6 eV, which is less than the experimental optical band gap of 3.0 eV.[73] We expect, however, that the DFT excitation energies of the unoccupied states with respect to the CBM do not suffer from the same errors as the quasiparticle gap.[74]

Considering the adsorbate-localized DOS, we note that the highest-occupied molecular orbital (HOMO) of the three structures, as reported in Table I, is just below the valance-

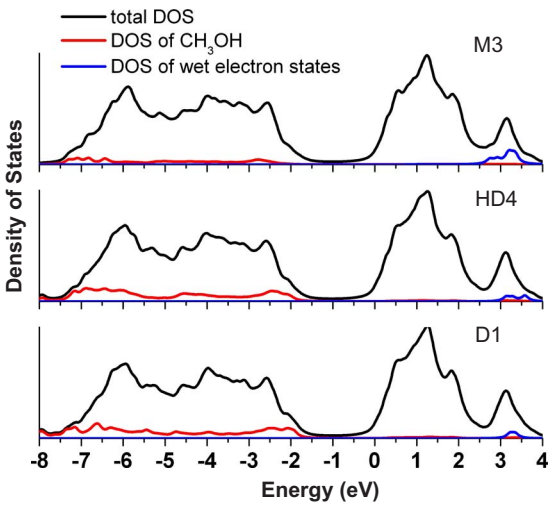

FIG. 5. (Color online) The total (black) and partial (red and blue) DOS for the M3, HD4, and D1 structures. The reference energy is the conduction-band minimum.

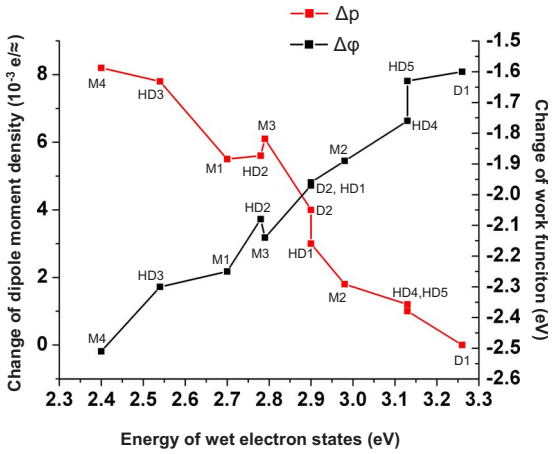

FIG. 6. (Color online) The correlation of the wet-electron energy for different adsorption structures with work-function change and the relative surface dipole moment.

band maximum (VBM). By contrast, the HOMO of H_2O is more than 5 eV below VBM.[61–65,75,76] This result is consistent with CH_3OH being a hole scavenger.[10] If we compare in detail the adsorbate localized DOS of the three structures, it is evident from Fig. 5 that the methoxy contribution is closer to VBM and has larger DOS than the methanol contribution. The deprotonation accumulates more electron charge density on O atom of methoxy raising its energy with respect to CH_3OH. Based on these results, it is evident that on CH_3OH-covered TiO_2-surface methoxy is the more favorable hole-trapping site than methanol. This suggests that trapping of photogenerated holes may provide the thermodynamic driving potential for proton transfer from CH_3OH to the substrate.

Chemisorption-induced charge transfer also affects the work function of CH_3OH/TiO_2 surfaces. We have calculated the work functions for the bare $TiO_2(110)$ surface and different structures of 1 ML CH_3OH chemisorbed on TiO_2 using the 11-layer slab by subtracting the calculated E_F from the vacuum level energy obtained from the analysis of the electrostatic potential. For the bare TiO_2 surface, the work function we obtain is 6.82 eV with respect to VBM, which is comparable to previous theoretical results.[77–80] The GGA band gap of TiO_2 being approximately 1.6 eV, locates the vacuum level at ~5.2 eV above CBM. In 2PP measurements, the work function is strongly surface-preparation dependent but for a stoichiometric surface it was reported to be 5.6 eV.[70] In other photoemission experiments it was found to be 5.3 eV.[81] The experimental work function suggests, therefore, that the GGA valence band may be as much as 0.1–0.4 eV too high.

Because of the uncertainty in the absolute value of work function, in Table I and Fig. 6 we report the chemisorption-induced work-function change relative to the bare surface. The calculated reduction in the work function by adsorption of 1 ML CH_3OH is 1.6–2.3 eV depending on the adsorption

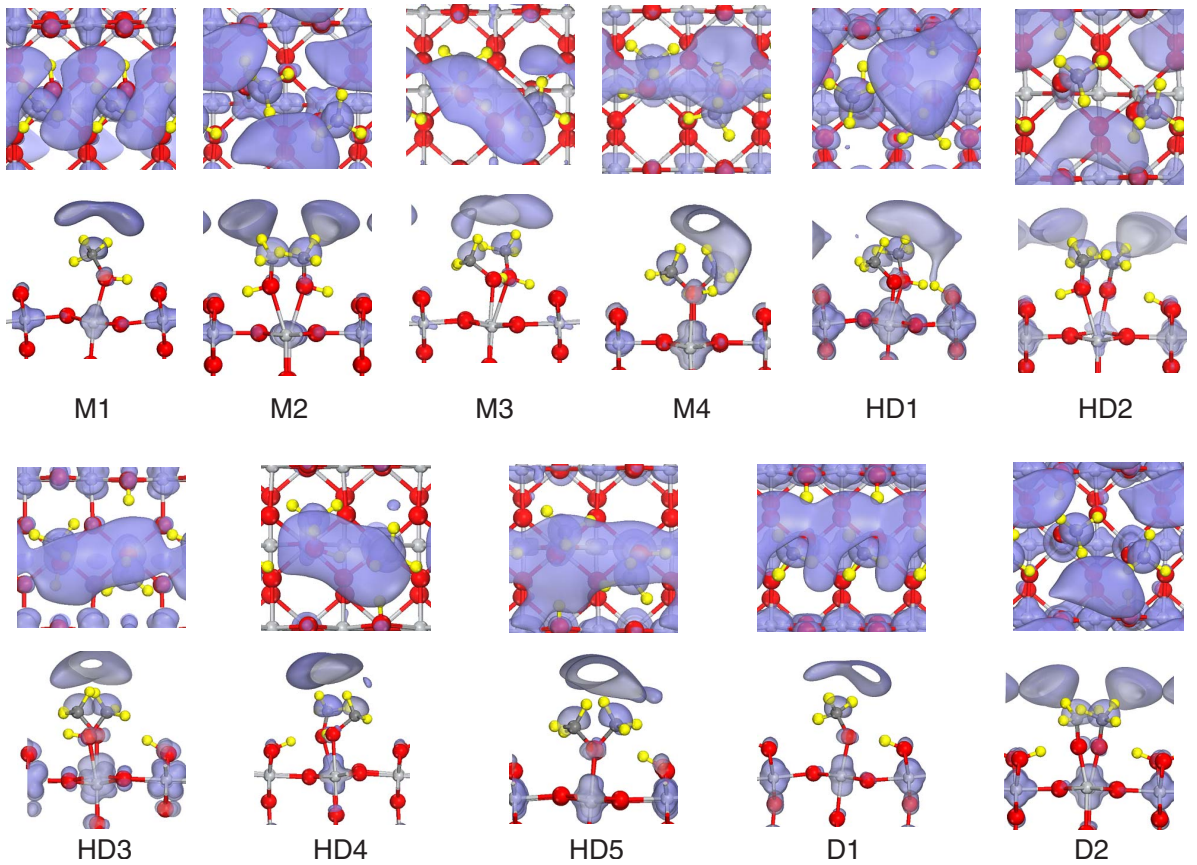

FIG. 7. (Color online) The top and side views of the spatial distribution of wet-electron orbitals for the different adsorption structures for 1 ML CH_3OH on TiO_2.

structure. The large variation in the work function is not associated with the molecular vs deprotonated chemisorption; rather it is associated with more subtle structural motifs. The work-function change in 2PP measurements on the stoichiometric $TiO_2(110)$ surface was found to be 1.2 eV.[18] The lower experimental value may reflect that the actual CH_3OH coverage for the nominally 1 ML structure corresponds to the filling of only 70% Ti_{5c} sites.[12]

The work-function change is strongly correlated with the surface dipole moment.[82,83] From the slab model calculation, we can define the density of dipole moment of the surface layer by $p=\int_{z_0}^{c/2} z\rho(z)dz$,[27,84,85] where c is the cell parameter (thickness of the slab plus vacuum) in the z direction. The center of the slab is taken as the starting point of the integration z_0 as dictated by symmetry. We note that our procedure allows us to obtain only the relative dipole values because the slab thickness is not sufficient to represent the long-range electrostatic forces required for convergence in determination of the absolute value of the dipole moment. Nevertheless, the relative values reported in Table I for different structures still provide useful information. We report surface dipole moments in Table I and Fig. 6 relative to the D1 structure, for which it is set to zero. The D1 structure has the smallest surface dipole moment, and therefore, induces the smallest change in the work function.

C. Wet-electron states

Motivated by the discovery of the CH_3OH-induced wet-electron states in TR-2PP experiments,[19] we examined the calculated unoccupied electronics structure associated with CH_3OH overlayer on of $TiO_2(110)$ surface. In the analysis of the unoccupied DOS, we find contributions from the diffuse states of the methanol overlayer that appear at adsorption structure-dependent energies. Because these states are predominantly associated with the adsorbate H atoms, we associate them with the wet-electron states. The unoccupied DOS in Fig. 5 indicates the wet-electron states of the representative M3, HD4, and D1 structures. The energy of the lowest wet-electron state with respect to CBM reported in Table I is defined as described in Ref. 27.

We note that the wet-electron-state energies of different adsorption structures fall in a relatively narrow range between 2.4 and 3.3 eV above the CBM. The M4 and D1 structures have the lowest and the highest wet-electron energies of 2.40 and 3.3 eV, respectively. In Fig. 7 we plot the spatial distributions of the wet-electron-state orbitals. For every adsorption structure, the wet-electron state is distributed mostly on top of H atoms of the methyl groups. The reason why H atoms of OH groups have only a minor contribution to the wet-electron states is that in most structures it forms strong molecule-surface or intermolecular HBs. The only exception is M4, where the HB from the OH in CH_3OH to the bridging O is rather weak as judged by its 2.42 Å bond length. Therefore, in this case the hydroxyl H atom can be considered a favorable dangling acceptor site that helps to stabilize the wet-electron state. A more general trend, however, can be discerned in Fig. 6, where we compare the relationship between the wet-electron-state energy and the work-function change; we find that a low wet-electron-state energy requires a high dipole density, and therefore is associated with a large work-function change.

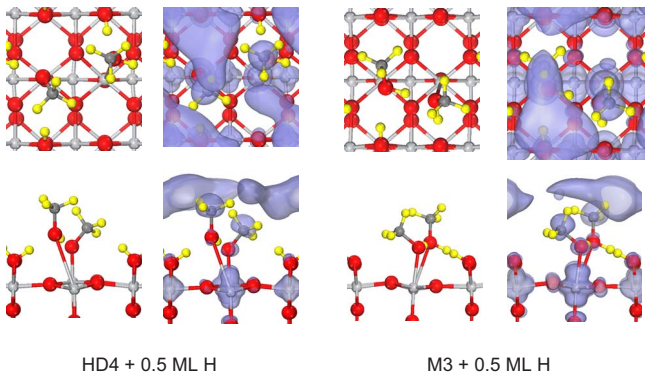

FIG. 8. (Color online) The top and side views of the spatial distribution of wet-electron orbitals for HD4 and M3 structures with additional 0.5 ML H of atoms added to the O_b sites.

In order to examine further the correlation of wet-electron states with the dipole moment, we have also examined the effect of adding 0.5 ML of H atoms to the M3 and HD4 structures. These structures are shown in Fig. 8 along with the wet-electron orbital distributions. Such OH_b species are expected on partially reduced TiO_2 surfaces on account of molecular dissociation of impurity H_2O and CH_3OH at O_b-atom vacancy defects. As described in our previous work on H_2O-covered TiO_2 surfaces,[27] H atoms at O_b sites transfer their valance electrons to Ti $3d$ states.[86] Through this charge transfer, H atoms contribute to the surface dipole moment. By increasing the dipole-moment density in this way, the energies of wet-electron states are reduced to 2.17 and 2.01 eV for the M3 and HD4 structures with the additional 0.5 ML of H atoms. The wet-electron-state energy decrease for the HD4 structure is 1.12 eV, which is larger than 0.62 eV for the M3 structure. This large energy stabilization can be in part attributed to formation of a dangling H atom on the surface. We note that adding 0.5 ML H to the HD4 structure causes the CH_3OH molecule in the unit cell to form intermolecular and molecule-surface HBs at the cost of dissociating the HB between methoxy and OH_b. Consequently, OH_b remains dangling making it a favorable wet-electron acceptor site. We note that in structures with intermolecular HBs one of the adsorbates within the unit cell is subject to two HBs. Adding 0.5 ML of H atoms to 1 ML of methanol allows each adsorbate within the unit cell to potentially have two HBs. The strain associated with such structures, however, is too large causing one of H atoms to remain dangling. Thus, on reduced TiO_2 surfaces, the formation of additional OH_b species will introduce the dangling H-atom sites that effectively stabilize wet electrons. This prediction is consistent with 2PP measurements of wet-electron states for the stoichiometric and reduced TiO_2 surfaces.[18,19]

IV. DISCUSSION

The question of whether the CH_3OH dissociates or not on stoichiometric $TiO_2(110)$ surface has been of considerable

interest.[8,12,16,17,22] Distinct features at 295 and 350 K in TPD scans for multilayer CH_3OH films on reduced $TiO_2(110)$ surface have been attributed, respectively, to the molecular and deprotonated species, which desorb from Ti_{5c} sites as CH_3OH molecules. Single-molecule-resolved STM measurements by Dohnálek and coworkers at room temperature show that CH_3OH molecules can diffuse along the Ti_{5c} rows without dissociating until they encounter an O_b vacancy site. The defect-induced dissociation introduces H and CH_3 species on top of O_b rows. According to the TPD measurements, desorption of these dissociated species from O_b rows occurs at even higher temperature of 400–550 K.[12] The STM measurements of Dohnélek and coworkers, however, were performed at a very low coverage where intermolecular interaction between proximate CH_3OH molecules could not influence the chemisorbed state.[23] According to our calculations, the intermolecular interactions can substantially alter stability of the molecular versus dissociated species. In a calculation for TiO_2 slabs with four to six layers for similar structure to our M1 structure, but at 0.25 ML coverage, de Armas *et al.*[17] found that whether the molecular or dissociated form of CH_3OH is more stable depends on the number of layers that are used in the calculation. Nudged elastic-band calculations from the same group for a six-layer slab show that the molecular adsorption is more stable by 0.02 eV than the corresponding deprotonated structure, and barrier to the interconversion is 0.11 eV. One should keep in mind, however, that these results are not converged with respect to the slab thickness.

The main result of our study on the relative chemisorption energies at 1 ML coverage of CH_3OH on $TiO_2(110)$ surface is that the intermolecular HB is very important to stabilize the adsorption. Based on our 11-layer slab calculation, the most stable structure corresponds to the molecular adsorption M3, which forms one intermolecular and another molecule-surface HB. Transferring the proton across the molecule-surface HB to O_b row transforms the M3 structure into the HD4 structure, which is less stable by 0.08 eV. The fully intermolecularly hydrogen-bonded methanol chains, which could mediate Grotthuss-type proton transport on the surface,[87–90] are not stable because of the steric hindrance of methyl groups.

Our study shows that for CH_3OH on TiO_2 there are many possible related adsorption structures with nearly equal adsorption energies for the molecular and deprotonated forms, for example, M2, HD2, and HD3. The molecular M3 structure is clearly the most stable structure, but for other nearly as stable structures, such as the M4 and HD5, the deprotonated form is predicted to be the more stable one. Thus, the extent to which methanol exists in a deprotonated form on CH_3OH/TiO_2 surface depends on the details of potential-energy surfaces for the interconversion of structures such as M4 transforming either into the deprotonated HD5 structure or the most stable M3 structure. Because the energy differences between the five most stable structures is <0.2 eV, it is likely that $CH_3OH/TiO_2(110)$ surfaces are highly inhomogeneous and contain a distribution of the structural motifs that arise from deprotonation, intermolecular, and molecule-substrate HBs, and possible H-atom migration that we have not discussed explicitly. The interconversion between different forms could be catalyzed by species such as OH_b or impurity H_2O molecules, and even by photogenerated holes.[91] Although the assignment of the TPD features at 295 and 350 K to the molecular and deprotonated forms of CH_3OH is plausible, in light of our finding of different stability of the intermolecular and molecule-surface HBs, the two features could also be attributed to differences in HB strengths of different molecular chemisorption structures.

We note that Henderson *et al.*[12] found 1 ML CH_3OH coverage to correspond to only 70% of the surface Ti_{5c} sites. To explain this, they proposed that on account of steric hindrance between the methyl groups one CH_3OH molecule within the 2×1 unit cell occupies a Ti_{5c} site while the other molecule adsorbs in a bridging site between two Ti_{5c} sites. Our calculations show that the steric hindrance is indeed an important factor in determining the CH_3OH overlayer structure but there is no stable adsorption minimum at the proposed bridging site. The steric hindrance between methyl groups, however, can cause some of the Ti_{5c} sites to be blocked, resulting in a monolayer coverage that is significantly less dense than if all the Ti_{5c} sites were available.

Our DFT study for the stoichiometric TiO_2 surface gives the wet-electron-state energy of different structures in the 2.4–3.3 eV range above CBM, which is consistent with the experimental 2PP spectra. The wet-electron-state energies do not show much sensitivity to whether CH_3OH is deprotonated or not. Adding 0.5 ML of H atoms onto O_b rows to simulate the situation that would exist on reduced surfaces, such as used in Refs. 19 and 56 reduces the wet-electron-state energy to the 2.0–2.2 eV range. Thus, the calculated wet-electron-state energies for the stoichiometric or reduced surfaces are entirely consistent with the experimental observation of a peak at 2.3 eV with a 0.6 eV width. The experimental width most likely reflects the inhomogeneity of methanol adsorption structures and the structure-dependent resonance energies.

For H_2O adsorbed on TiO_2, the possibility of having both intermolecular and molecule-surface HBs leaves no dangling H atoms as acceptor sites. Therefore, the OH_b species on reduced surfaces provide the primary dangling H-atom sites, which bring the wet-electron-state energy down to 2.4 eV above E_F.[27] For CH_3OH on the stoichiometric TiO_2 surface, the wet-electron-state density is distributed mainly on H atoms of the methyl groups. Because CH_3OH can make only one HB per molecule, any extra OH_b species formed either by deprotonation or methanol dissociation at O_b vacancy defect sites form strong HBs with short bond lengths with O atoms of methanol or methoxy at Ti_{5c} sites; therefore, OH_b species are not favorable acceptor sites in a vertical photoinduced charge transfer. Rather, our calculations show that the less acidic methyl H atoms are the more favorable electron acceptor sites. Methyl H atoms offer multiple acceptor sites that cannot participate in HBs, making them superior for stabilizing the diffuse wet-electron orbitals that the more acidic hydrogen-bonded OH species. The propensity for electron solvation by methyl H atoms has also been found in calculations on methanol clusters.[69]

Instead of the defect-induced formation of OH_b species on H_2O/TiO_2 surfaces,[27] the wet-electron energy in the case of CH_3OH/TiO_2 surface is mostly determined by the surface

dipole moment, as can be seen in Fig. 6. This is consistent with the previous studies on H_2O clusters, where the dipolar forces define the wet-electron binding energy.[38,40,92] Although adding 0.5 ML of OH_b to CH_3OH/TiO_2 surface lowers the wet-electron-state energy, the main role of OH_b is to increase the surface dipole moment. The additional OH_b species form HBs with methanol and methoxy species, rather than remaining as dangling H-atom acceptor sites. Because of this sensitivity on the surface dipole moment, at the solid-liquid interface we expect the acidic conditions to favor the stabilization the wet-electron states for CH_3OH-covered TiO_2 surfaces.

The wet-electron states for H_2O and CH_3OH on $TiO_2(110)$ surface have been recently investigated by DFT calculations using atomic basis sets.[93] The results obtained and conclusions drawn are significantly different from our 2PP experiments[19,56] and the present theoretical work. Using the double zeta and polarization (DZP) and DZP++ basis sets, Koitaya *et al.* obtained much higher wet-electron-state energies for both H_2O/TiO_2 and CH_3OH/TiO_2 surfaces. For instance, they report the wet-electron-state energy for the molecular and dissociated CH_3OH structures at 1 ML to be $\geq$4.9 eV. The discrepancy with our calculations can be attributed to (i) their reference energy E_F being located apparently about 1 eV below CBM whereas experimental one is only $\sim$120 meV below the CBM (Refs. 19, 56, and 70); and more importantly, (ii) their atomic basis sets not being sufficiently diffuse to describe accurately wet-electron states. Koitaya *et al.* found that the more diffuse DZP++ basis can reduce the wet-electron-state energy by as much as 0.7 eV with respect to the DZP basis sets. Other theoretical studies have investigated the convergence of diffuse solvated electron states on surfaces of H_2O clusters with respect to the size of basis sets employed.[94–98] For instance, Kim *et al.* have shown that at least a TZ2P++ basis set is required to describe H_2O anion clusters.[98] Tellingly, the much higher-energy wet-electron states found by Koitaya *et al.* are mainly associated with OH_b species, which in our calculations do not support the lowest-energy wet-electron states. The plane-wave basis set we are using is nearly complete, and therefore, we believe provides better description of the diffuse wet-electron states associated with H atoms of methyl groups than a more limited atomic basis set such as DZP++.

In summary, we have investigated the adsorption structures and wet-electron states of 1 ML CH_3OH adsorbed on rutile $TiO_2(110)$ surface. Among the 11 stable structures we have found, the molecular adsorption M3 and half-dissociated HD3 and HD4 structures with intermolecular HBs are the most stable ones. The wet-electron states distribute mostly on the H atoms of methyl groups, rather than the more acidic OH species, which are engaged in strong HBs. The wet-electron-state energies for different structures are strongly correlated with the surface dipole moment. Because different methanol structures have similar wet-electron-state energies, the molecular response to the injection of charge into the wet-electron state might be very complicated and structure dependent. To investigate the solvation dynamics of excited wet electrons on CH_3OH/TiO_2 interface, theoretical methods beyond DFT, which can treat the excited electron dynamics including adiabatic and nonadiabatic electron transfer will need to be used.[99–101]

ACKNOWLEDGMENTS

This work was funded through grants from ARO (Grant No. W911NF-07-1-0052) and NSF (Grant No. CHE-0650756). Calculations were performed in the Environmental Molecular Sciences Laboratory at the Pacific Northwest National Laboratory, a user facility sponsored by the DOE Office of Biological and Environmental Research.

[1] A. Fujishima and K. Honda, Nature (London) **238**, 37 (1972).
[2] M. Grätzel, Comments Inorg. Chem. **12**, 93 (1991).
[3] A. L. Linsebigler, G. Lu, and J. J. T. Yates, Chem. Rev. (Washington, D.C.) **95**, 735 (1995).
[4] U. Diebold, Surf. Sci. Rep. **48**, 53 (2003).
[5] A. Fujishima, X. Zhang, and D. A. Tryk, Surf. Sci. Rep. **63**, 515 (2008).
[6] G. E. Brown, Jr., V. E. Henrich, W. H. Casey, D. L. Clark, C. Eggleston, A. Felmy, D. W. Goodman, M. Grätzel, G. Maciel, M. I. McCarthy, K. H. Nealson, D. A. Sverjensky, M. F. Toney, and J. M. Zachara, Chem. Rev. **99**, 77 (1999).
[7] L. Gundlach, R. Ernstorfer, and F. Willig, Prog. Surf. Sci. **82**, 355 (2007).
[8] S. P. Bates, M. J. Gillan, and G. Kresse, J. Phys. Chem. B **102**, 2017 (1998).
[9] S. P. Bates, G. Kresse, and M. J. Gillan, Surf. Sci. **409**, 336 (1998).
[10] T. L. Thompson and J. T. Yates, J. Phys. Chem. B **109**, 18230 (2005).
[11] M. A. Henderson, S. Otero-Tapia, and M. E. Castro, Surf. Sci. **412-413**, 252 (1998).
[12] M. A. Henderson, S. Otero-Tapia, and M. E. Castro, Faraday Discuss. **114**, 313 (1999).
[13] C.-C. Chuang, C.-C. Chen, and J.-L. Lin, J. Phys. Chem. B **103**, 2439 (1999).
[14] R. Tero, K. Fukui, and Y. Iwasawa, J. Phys. Chem. B **107**, 3207 (2003).
[15] A. Tilocca and A. Selloni, J. Phys. Chem. B **108**, 19314 (2004).
[16] Z. Zhang, O. Bondarchuk, J. M. White, B. D. Kay, and Z. Dohnalek, J. Am. Chem. Soc. **128**, 4198 (2006).
[17] R. Sánchez de Armas, J. Oviedo, M. Á. San Miguel, and J. F. Sanz, J. Phys. Chem. C **111**, 10023 (2007).
[18] K. Onda, B. Li, J. Zhao, and H. Petek, Surf. Sci. **593**, 32 (2005).
[19] B. Li, J. Zhao, K. Onda, K. D. Jordan, J. Yang, and H. Petek, Science **311**, 1436 (2006).
[20] G. S. Herman, Z. Dohnálek, N. Ruzycki, and U. Diebold, J. Phys. Chem. B **107**, 2788 (2003).
[21] E. Farfan-Arribas and R. J. Madix, Surf. Sci. **544**, 241 (2003).
[22] J. Oviedo, R. Sánchez de Armas, M. Á. San Miguel, and J. F. Sanz, J. Phys. Chem. C **112**, 17737 (2008).
[23] Z. Zhang, O. Bondarchuk, B. D. Kay, J. M. White, and Z. Dohnalek, J. Phys. Chem. C **111**, 3021 (2007).

[24] L.-M. Liu, P. Crawford, and P. Hu, Prog. Surf. Sci. **84**, 155 (2009).
[25] T. Kawai and T. Sakata, J. Chem. Soc., Chem. Commun. **694** (1980).
[26] A. Yamakata, T. Ishibashi, and H. Onishi, J. Phys. Chem. B **106**, 9122 (2002).
[27] J. Zhao, B. Li, K. D. Jordan, J. Yang, and H. Petek, Phys. Rev. B **73**, 195309 (2006).
[28] J. Zhao, B. Li, K. Onda, M. Feng, and H. Petek, Chem. Rev. (Washington, D.C.) **106**, 4402 (2006).
[29] K. S. Kim, I. J. Park, S. Lee, K. Cho, J. Y. Lee, J. Kim, and J. D. Joannopoulos, Phys. Rev. Lett. **76**, 956 (1996).
[30] J. Schnitker, K. Motakabbir, P. J. Rossky, and R. A. Friesner, Phys. Rev. Lett. **60**, 456 (1988).
[31] J. V. Coe, G. H. Lee, J. G. Eaton, S. T. Arnold, H. W. Sarkas, K. H. Bowen, C. Ludewigt, H. Haberland, and D. R. Worsnop, J. Chem. Phys. **92**, 3980 (1990).
[32] A. Staib and D. Borgis, J. Chem. Phys. **103**, 2642 (1995).
[33] A. Wallqvist, G. Martyna, and B. J. Berne, J. Phys. Chem. **92**, 1721 (1988).
[34] C. Silva, P. K. Walhout, K. Yokoyama, and P. F. Barbara, Phys. Rev. Lett. **80**, 1086 (1998).
[35] M. Boero, M. Parrinello, K. Terakura, T. Ikeshoji, and C. C. Liew, Phys. Rev. Lett. **90**, 226403 (2003).
[36] H. Haberland, C. Ludewigt, H.-G. Schindler, and D. R. Worsnop, J. Chem. Phys. **81**, 3742 (1984).
[37] K. D. Jordan, Science **306**, 618 (2004).
[38] K. D. Jordan and F. Wang, Annu. Rev. Phys. Chem. **54**, 367 (2003).
[39] L. Turi, W. S. Sheu, and P. J. Rossky, Science **309**, 914 (2005).
[40] C. G. Zhan and D. A. Dixon, J. Phys. Chem. B **107**, 4403 (2003).
[41] E. J. Hart and J. W. Boag, J. Am. Chem. Soc. **84**, 4090 (1962).
[42] J. P. Keene, Nature (London) **197**, 47 (1963).
[43] L. Kevan, Acc. Chem. Res. **14**, 138 (1981).
[44] R. N. Barnett, U. Landman, C. L. Cleveland, and J. Jortner, J. Chem. Phys. **88**, 4429 (1988).
[45] N. I. Hammer, J.-W. Shin, J. M. Headrick, E. G. Diken, J. R. Roscioli, G. H. Weddle, and M. A. Johnson, Science **306**, 675 (2004).
[46] J. W. Shin, N. I. Hammer, E. G. Diken, M. A. Johnson, R. S. Walters, T. D. Jaeger, M. A. Duncan, R. A. Christie, and K. D. Jordan, Science **304**, 1137 (2004).
[47] A. E. Bragg, J. R. R. Verlet, A. Kammrath, O. Cheshnovsky, and D. M. Neumark, Science **306**, 669 (2004).
[48] J. R. R. Verlet, A. E. Bragg, A. Kammrath, O. Cheshnovsky, and D. M. Neumark, Science **307**, 93 (2005).
[49] D. H. Paik, I. R. Lee, D. S. Yang, J. S. Baskin, and A. H. Zewail, Science **306**, 672 (2004).
[50] M. Skorobogatiy, I. J. Park, and J. D. Joannopoulos, Comput. Mater. Sci. **32**, 96 (2005).
[51] F. Baletto, C. Cavazzoni, and S. Scandolo, Phys. Rev. Lett. **95**, 176801 (2005).
[52] C. Gahl, U. Bovensiepen, C. Frischkorn, and M. Wolf, Phys. Rev. Lett. **89**, 107402 (2002).
[53] U. Bovensiepen, Prog. Surf. Sci. **78**, 87 (2005).
[54] J. Stähler, U. Bovensiepen, M. Meyer, and M. Wolf, Chem. Soc. Rev. **37**, 2180 (2008).
[55] U. Bovensiepen, C. Gahl, J. Stähler, M. Bockstedte, M. Meyer, F. Baletto, S. Scandolo, X.-Y. Zhu, A. Rubio and M. Wolf, J. Phys. Chem. C **113**, 979 (2009).
[56] K. Onda, B. Li, J. Zhao, K. D. Jordan, J. Yang, and H. Petek, Science **308**, 1154 (2005).
[57] T. L. Thompson and J. T. Yates, Jr., Chem. Rev. (Washington, D.C.) **106**, 4428 (2006).
[58] J. P. Perdew, K. Burke, and M. Ernzerhof, Phys. Rev. Lett. **77**, 3865 (1996).
[59] G. Kresse and D. Joubert, Phys. Rev. B **59**, 1758 (1999).
[60] P. M. Kowalski, B. Meyer, and D. Marx, Phys. Rev. B **79**, 115410 (2009).
[61] D. Vogtenhuber, R. Podloucky, and J. Redinger, Surf. Sci. **402-404**, 798 (1998).
[62] E. V. Stefanovich and T. N. Truong, Chem. Phys. Lett. **299**, 623 (1999).
[63] R. L. Kurtz, R. Stockbauer, T. E. Madey, E. Roman, and J. De Segovia, Surf. Sci. **218**, 178 (1989).
[64] P. J. D. Lindan and C. Zhang, Phys. Rev. B **72**, 075439 (2005).
[65] S. Krischok, J. A. Schaefer, O. Höfft, and V. Kempter, Surf. Interface Anal. **37**, 83 (2005).
[66] N. A. Deskins, Chem. Phys. Lett. **471**, 75 (2009).
[67] See EPAPS Document No. E-PRBMDO-80-136943 for Bader analysis of Charge. For more information on EPAPS, see http://www.aip.org/pubservs/epaps.html.
[68] H. Kamisaka and K. Yamashita, Surf. Sci. **601**, 4824 (2007).
[69] L. Turi, J. Chem. Phys. **110**, 10364 (1999).
[70] K. Onda, B. Li, and H. Petek, Phys. Rev. B **70**, 045415 (2004).
[71] M. Aono and R. R. Hasiguti, Phys. Rev. B **48**, 12406 (1993).
[72] A. Yamakata, T. Ishibashi, and H. Onishi, J. Mol. Catal. A: Chem. **199**, 85 (2003).
[73] A. Amtout and R. Leonelli, Phys. Rev. B **51**, 6842 (1995).
[74] X. Lu, M. Grobis, K. H. Khoo, S. G. Louie, and M. F. Crommie, Phys. Rev. B **70**, 115418 (2004).
[75] J. Goniakowski and M. J. Gillan, Surf. Sci. **350**, 145 (1996).
[76] I. M. Brookes, C. A. Muryn, and G. Thornton, Phys. Rev. Lett. **87**, 266103 (2001).
[77] D. Vogtenhuber, R. Podloucky, A. Neckel, S. G. Steinemann, and A. J. Freeman, Phys. Rev. B **49**, 2099 (1994).
[78] D. Vogtenhuber, R. Podloucky, and J. Redinger, Surf. Sci. **454-456**, 369 (2000).
[79] D. Vogtenhuber, R. Podloucky, J. Redinger, E. L. D. Hebenstreit, W. Hebenstreit, and U. Diebold, Phys. Rev. B **65**, 125411 (2002).
[80] J. R. B. Gomes and J. P. Prates Ramalho, Phys. Rev. B **71**, 235421 (2005).
[81] A. W. Grant and C. T. Campbell, Phys. Rev. B **55**, 1844 (1997).
[82] G. A. Somorjai, *Introduction to Surface Chemistry and Catalysis* (Wiley, New York, 1994).
[83] A. Zangwill, *Physics at Surfaces* (Cambridge University Press, Cambridge, 1988).
[84] G. Materzanini, G. F. Tantardini, P. J. D. Lindan, and P. Saalfrank, Phys. Rev. B **71**, 155414 (2005).
[85] T. C. Leung, C. L. Kao, W. S. Su, Y. J. Feng, and C. T. Chan, Phys. Rev. B **68**, 195408 (2003).
[86] T. Minato, Y. Sainoo, Y. Kim, H. S. Kato, K.-i. Aika, M. Kawai, J. Zhao, H. Petek, T. Huang, W. He, B. Wang, Z. Wang, Y. Zhao, J. Yang, and J. G. Hou, J. Chem. Phys. **130**, 124502 (2009).
[87] H. C. Chang, J. C. Jiang, S. H. Lin, and Y. T. Lee, J. Phys. Chem. A **103**, 2941 (1999).
[88] F. C. Hagemeister, C. J. Gruenloh, and T. S. Zwier, J. Phys. Chem. A **102**, 82 (1998).

[89] J. A. Morrone and M. E. Tuckerman, J. Chem. Phys. **117**, 4403 (2002).
[90] E. S. Stoyanov, I. V. Stoyanova, and C. A. Reed, Chemistry (Weinheim, Ger.) **14**, 3596 (2008).
[91] Z. Zhang, Y. Du, N. G. Petrik, G. A. Kimmel, I. Lyubinetsky, and Z. Dohnálek, J. Phys. Chem. C **113**, 1908 (2009).
[92] S. Lee, J. Kim, S. J. Lee, and K. S. Kim, Phys. Rev. Lett. **79**, 2038 (1997).
[93] T. Koitaya, H. Nakamura, and K. Yamashita, J. Phys. Chem. C **113**, 7236 (2009).
[94] J. G. C. M. D.-d. Rijdt and F. B. v. Duijneveldt, J. Chem. Phys. **97**, 5019 (1992).
[95] K. Kim and K. D. Jordan, J. Phys. Chem. **98**, 10089 (1994).
[96] E. M. Mas and K. Szalewicz, J. Chem. Phys. **104**, 7606 (1996).
[97] M. Schütz, S. Brdarski, P.-O. Widmark, R. Lindh, and G. Karlström, J. Chem. Phys. **107**, 4597 (1997).
[98] J. Kim and K. S. Kim, J. Chem. Phys. **109**, 5886 (1998).
[99] O. V. Prezhdo, W. R. Duncan, and V. V. Prezhdo, Prog. Surf. Sci. **84**, 30 (2009).
[100] S. A. Fischer, W. R. Duncan, and O. V. Prezhdo, J. Am. Chem. Soc. **131**, 15483 (2009).
[101] C. Venkataraman, A. V. Soudackov, and S. Hammes-Schiffer, J. Chem. Phys. **131**, 154502 (2009).